Microplastic Entrainment in Hail: Uncovering New Pathways for Atmospheric Pollution

Thomas Nordstrand

thomas.nordstrand@yahoo.com

Umiversity of Texas at San Antonio https://orcid.org/0000-0003-0396-238X

Yongli Gao

University of Texas at San Antonio https://orcid.org/0000-0001-9063-4792

Stephen Ackley

University of Texas at San Antonio

Skylar O'connell

Andre Felton

Andrew Heymsfield

Janice Brahney

Utah State University https://orcid.org/0000-0001-7614-2855

John Allen

Anthony Bernal Ayala

Talia Kurtz

Article

Keywords:

Posted Date: May 27th, 2026

DOI: https://doi.org/10.21203/rs.3.rs-9512208/v1

Additional Declarations: There is **NO** Competing Interest.

Microplastic Entrainment in Hail: Uncovering New Pathways for Atmospheric Pollution

Thomas E. Nordstrand[1], Yongli Gao[1], Stephen F. Ackley[1], Skylar O'Connell[1], Andre Felton[2], Andy Heymsfield[3], Janice Brahney[4], John T. Allen[5], Anthony C. Bernal Ayala[6], Talia Kurtz[7]

[1]Department of Earth and Planetary Sciences, University of Texas at San Antonio, NASA Center for Advanced Measurement in Extreme Environments (CAMEE), San Antonio, TX, 78249 USA.
[2]Department of Integrated Biology, University of Texas at San Antonio, San Antonio, TX, 78249, USA.
[3]NSF National Center for Atmospheric Science, Boulder, CO, 80307 USA.
[4]Department of Watershed Sciences, Utah State University, Logan, UT, 84322, USA.
[5]Department of Earth and Atmospheric Sciences, Central Michigan University, Mount Pleasant MI, 48859, USA.
[6]Atmospheric and Environmental Research (AER), JANUS Research Group, Boulder, CO, 80301, USA.
[7]Department of Atmospheric Sciences, University of North Dakota, Grand Forks, ND, 58202, USA.
Corresponding author: Thomas E. Nordstrand (thomas.nordstrand@yahoo.com)

Key Points:

- Hailstones archive atmospheric microplastics from convective storm inflow air masses
- Fragments dominate hailstone microplastics; polycarbonate is the most common polymer
- Air-mass trajectories link microplastic sources to manufacturing zones and urban land-use

Abstract

Microplastics are recognized as a ubiquitous component of atmospheric particulate pollution, yet the inflow wind distribution, transport and accretion on hailstones within severe convective storm systems remain poorly understood. This study provides the first comprehensive analysis of microplastics preserved in hailstones from two major supercell storms in Texas: Del Rio (11 April 2020) and Uvalde (28 April 2021). Twenty-one hailstones were randomly chosen, melted,

filtered through Whatman 0.2µm membranes, and retained particles analyzed using Fourier-Transform Infrared (FTIR) microscopy for polymer identification and morphological characterization. Microplastics were detected in every hailstone (N = 283 particles), confirming their ubiquity in the lower troposphere. Fragments were dominant morphology (69.4%), followed by fibers (23.6%), films (6.6%), and spheres (0.4%). Fifty-eight distinct polymer species were identified, with polycarbonate (n = 87), epoxy (n = 23), and polybutadiene (n = 14) comprising the most abundant chemical classes. A Kruskal–Wallis H test (p = 0.0176) revealed statistically significant heterogeneity among hailstones, implying multiple emission sources and atmospheric transport histories. HYSPLIT back-trajectory and land-use analyses revealed that low-level inflow air masses traversed manufacturing zones along the U.S. Mexico border and urban population centers that contributed to microplastic loading within the storm systems. These findings demonstrate that convective storms effectively scavenge and archive airborne microplastics, offering a novel approach for assessing inflow air mass transport and emission patterns in the atmosphere. Hailstones represent an underutilized natural archive for evaluating emission sources, inflow air mass transport, monitoring microplastic pollution and contributing to the atmospheric microplastic body of knowledge.

Graphical Abstract

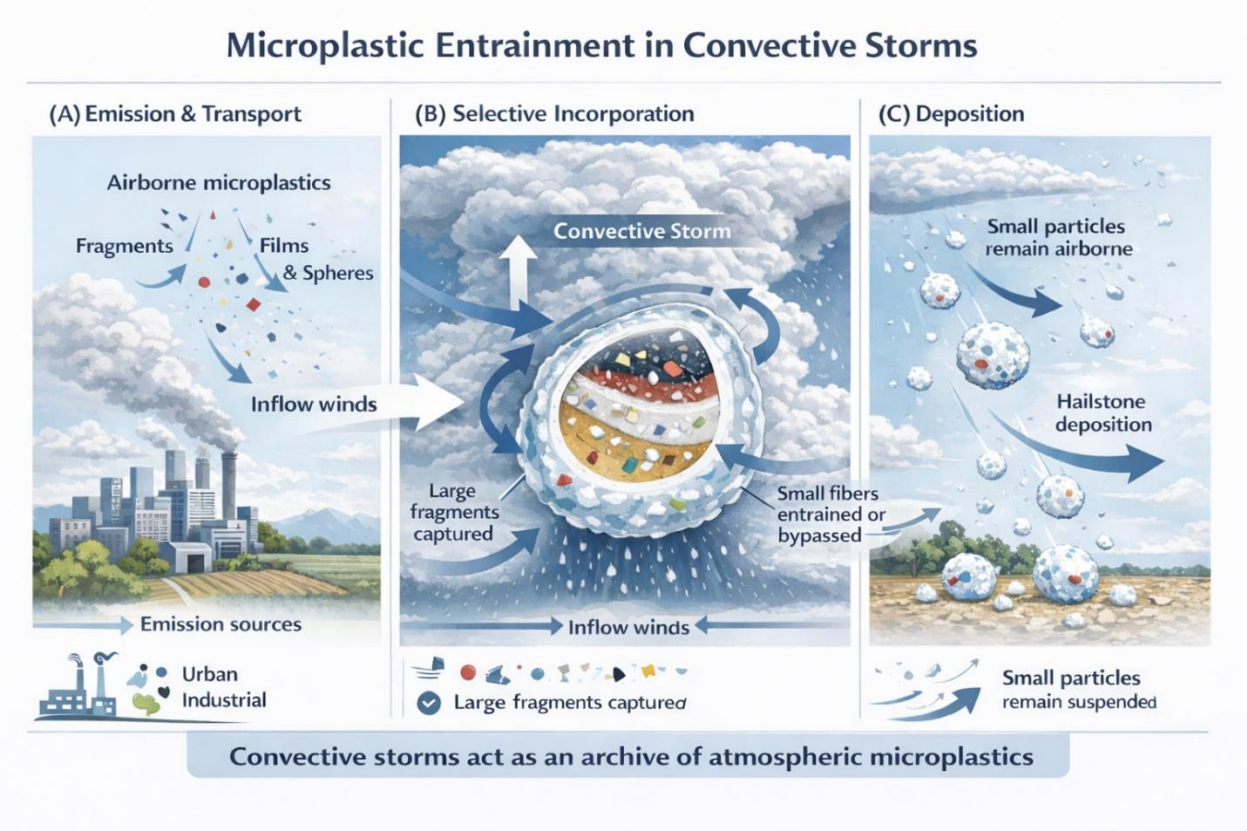

Plain Language Summary

This research shows that small plastic particles ranging in size from one micron to five millimeters, known as microplastics, are carried in the troposphere and are accreted onto hailstones during hail producing storms. Hailstones in excess of 2.54cm (1in) were analyzed from two supercell events in Texas and melted to determine if microplastics were present. Every hailstone analyzed in this study contained microplastics in the form of fragments, films or fibers.

The findings indicate that atmospheric microplastic pollution is ubiquitous including areas with low population density and industrial capacity. Winds transport these small plastic particles long distances where they eventually settle out because of gravity, rain or accretion onto hailstones. By studying the composition of hailstones, the atmospheric transport and potential origin of microplastic pollutants can be determined. This study highlights how anthropogenic air pollutants such as microplastics are recorded in hailstones that help us understand how they are transported and deposited in remote regions.

1.0 Introduction

Microplastics (MPs) are defined as any synthetic polymer (petrochemical) particle between 1μm and 5mm in size and have become a pervasive environmental pollutant throughout terrestrial, marine and atmospheric ecosystems (Dris et al., 2016; Hartmann et al., 2019; Rochman et al., 2019; Song et al., 2015; Thompson et al., 2004; Zhang et al., 2020). The low density and small size of MPs enable wide spatial distribution and atmospheric suspension, permitting access to remote geographies (Allen et al., 2019; Brahney et al., 2020; Camarero et al., 2017; Chen et al., 2020; Huang et al., 2021; Klein and Fischer, 2019). Airborne MPs interact with other aerosols, undergo degradation and return to the surface via dry deposition, precipitation or hydrometeors (Gasperi et al., 2018; Huang et al., 2021). Atmospheric MP pollution is ubiquitous raising concerns regarding their persistence, inhalation and role as an environmental pollutant (Peng et al., 2017; Prata, 2018; Worm et al., 2017).

Atmospheric MPs are derived from an array of anthropogenic sources, such as tire wear, textiles, emissions and degradation resulting from UV radiation and mechanical weathering (Cooper and

Corcoran, 2010; Law and Thompson, 2014; Steinmetz and Schröder, 2022). Land-use strongly influences MP emission: urban areas contribute through tire abrasion, emissions, construction and personal plastic pollution, while agricultural regions emit MPs via the fragmentation of plastic mulch, fertilizers and other agricultural inputs (Abbasi et al., 2019; Akca et al., 2024; Bi et al., 2023; Habib et al., 2022). The diverse sources of MPs produce fragment, film, fiber and sphere morphologies and a range of polymer types that are dispersed through the atmosphere by meteorological conditions (Allen et al., 2019; Cheung and Not, 2023; Klein and Fischer, 2019).

The presence of MPs in the atmosphere has been validated in snow, rain and aerosols (Bergmann et al., 2019; Brahney et al., 2020; Dris et al., 2017), however the vertical distribution, entrainment, and interactions with severe convective storms remain poorly understood. Hailstones formed in supercell thunderstorms provide a unique opportunity to investigate these processes. Hailstones grow via successive cycling in the updraft of supercell storms accreting water and entraining organic and inorganic particles present in the inflow boundary (Kozjek et al., 2023; Li et al., 2020; Nordstrand, 2021; Rochman et al., 2019; Šantl-Temkiv et al., 2013; Temkiv et al., 2012). Formed hailstones preserve a layered fingerprint of the atmospheric composition at the time of accretion, providing direct physical evidence of pollutants present in the troposphere.

Often termed “Hail Alley” the great plains of the United States, experiences frequent supercell storm events capable of producing large hail (>2.5cm) typically from April to July (Allen et al., 2020; Knight et al., 2019; Raupach et al., 2021). The coupling of meteorological conditions and microplastic sourcing, make the region ideal for investigation of MP entrainment and accretion

mechanisms. To our knowledge, no study has examined hailstones as proxies for environmental atmospheric MP pollution in the United States, nor evaluated the relationships between polymer type, morphology, and land-use emissions.

The presence and characteristics of MPs in hailstones collected from two major supercell events in Del Rio and Uvalde, Texas are investigated in this study. Fourier-transform infrared (FTIR) microscopy was used to identify polymer composition and morphology, while non-parametric statistics were applied to evaluate chemical heterogeneity among samples. Air mass back trajectory and land-use analyses were utilized to assess potential regional emission sources. The primary objectives of this study were to; quantify and characterize microplastics entrained in hailstones, assess differing polymer types and morphologies, and evaluate the contribution of land-use to microplastic loadings in the troposphere.

2. Background

Atmospheric MP identification and quantification remain a significant analytical and environmental challenge as the particle size decreases below 500µm. Early atmospheric MP studies relied on visual microscopy for identification of particles based on color and morphology (Araujo et al., 2018; Zhang et al., 2020). Detection thresholds and observer bias are limitations underscoring the need for spectroscopic confirmation. Chemical characterization using FTIR or Raman spectroscopy has become the standard for confirming polymer composition and anthropogenic origin (Hartmann et al., 2019; Stanton et al., 2019). The impact of MPs on ecosystems and human health require established protocols for the quantification of atmospheric microplastics.

The distribution and abundance of MPs in the atmosphere is influenced by emission sources, particle density, meteorological conditions, and land-use activities. Agricultural practices such as plastic mulch application, tillage, and fertilizer contribute to MP generation and redistribution through soil disturbance, runoff and aerosolization (Akca et al., 2024; Bi et al., 2023). Degradation of plastic mulch over time occurs due to ultraviolet radiation, temperature fluctuations, and mechanical stress, resulting in smaller fragments that can be transported by wind and incorporated into the atmosphere (Brahney et al., 2021; Steinmetz and Schröder, 2022). Likewise, urban environments emit MPs from vehicle tire wear, textile fibers, building materials, manufacturing emissions and individual person pollution (Habibi et al., 2024). The land-use and atmospheric interaction play a central role in regional emission and atmospheric MP pollution loading.

Despite widespread atmospheric MP contamination, data is sparse and spatially inconsistent across the United States. Previous research has focused on deposition in different environments and geographies leaving a significant deficiency in atmospheric MP analysis in particular vertical MP movement and entrainment into hydrometeors such as hailstones. Hailstone formation in convective clouds provide a unique mechanism by which atmospheric particles are accreted, preserved and archived during growth cycles (Kozjek et al., 2023; Šantl-Temkiv et al., 2013). The chemical and morphological characterization of MPs in hailstones can provide information on atmospheric pathways, origination of emissions, and impact of land-use on atmospheric MP concentration.

This study utilizes FTIR spectroscopy and Hybrid Single Particle Lagrangian Integrated Trajectory (HYSPLIT) back-trajectory to analyze MPs preserved in hailstones collected from two Texas supercell storms (Stein et al., 2015). By integrating polymer identification, morphology classification, and air-mass pathway modeling, the study aims to; characterize the composition and diversity of atmospheric MPs in hailstones, evaluate the spatial heterogeneity of MP chemical species, and assess the influence of land-use atmospheric MP emissions and deposition.

3.0 Materials and Methods

3.1 Sample collection

Hailstones were collected from Del Rio (GPS Coordinates: 29º 21’ 41” N 100º 53’ 59” W) and Uvalde (GPS coordinates: 29º 12’ 35” 99º 47’ 09” W) Texas on April 11, 2020 and April 28, 2021 respectively (Fig. 1) after the catastrophic hail events caused significant and widespread property damage. Sometime after falling eleven hailstones from Del Rio and ten hailstones from Uvalde ranging in size from 4.8cm (1.9in) to 8.2cm (3.2in) were collected by members of the community, placed in two sealed polyethylene bags to prevent sublimation and contamination. Hailstones were transported to the University of Texas at San Antonio (UTSA) Earth and Planetary Science Department in insulated coolers containing dry ice (-78.5ºC) and stored at -20ºC until analysis.

179

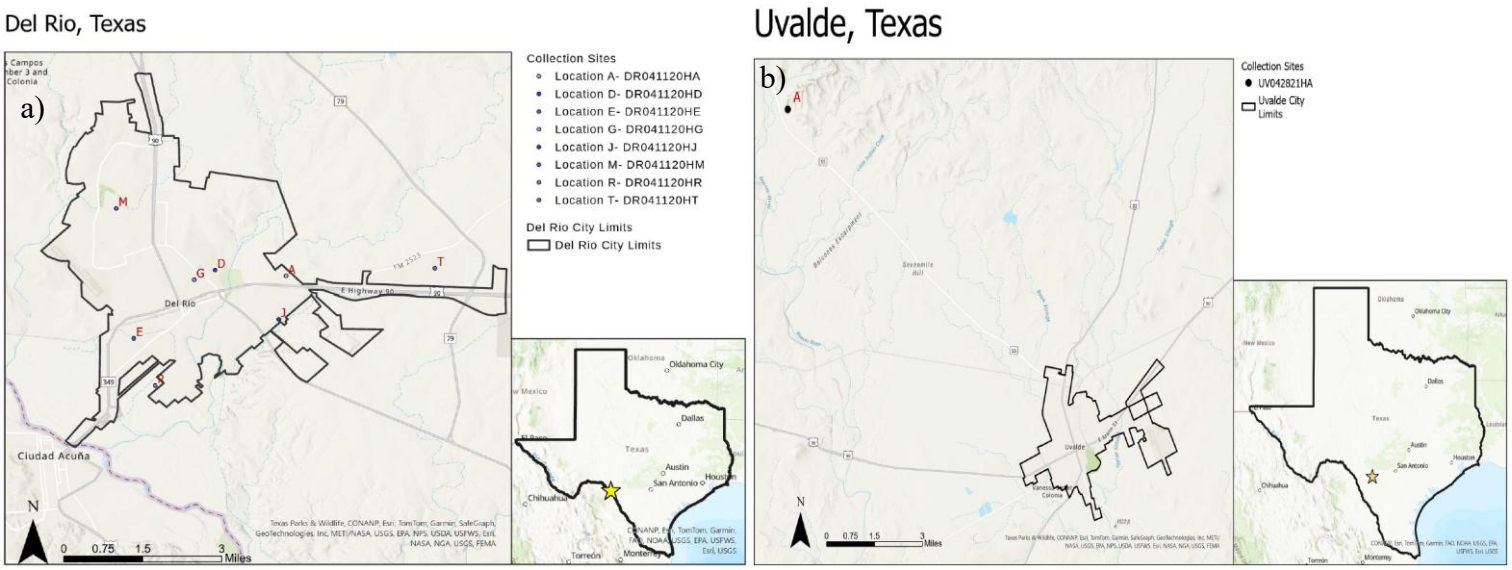

Figure 1. Hailstone collection locations for a) Del Rio Texas and b) Uvalde Texas.

180

181 Each Hailstone was measured along its three principal axes using Husky® caliper (± 0.02mm)
182 and measuring their mass with a Taylor® kitchen scale (± 0.1g) and were identified as being
183 triaxial ellipsoidal in shape. Their physical dimensions were recorded before and after cleaning
184 (Table 1). All handling and measurements were conducted in a clean laboratory environment to
185 minimize contamination.

186

187

Table 1. Physical attributes of hailstones before and after cleaning.

Sample	Mass Before Rinising (g)	Diameter Before Rinsing (mm) x	y	z	Mass After Rinising (g)	Diameter After Rinsing (mm) x	y	z	Mass Lost (g)
DR041120HA10	131	69.3	63.7	63.5	108	63.8	62.2	57.6	23
DR041120HA32	NR	NR	NR	NR	NR	NR	NR	NR	NR
DR041120HD03	91	69.6	58.6	47.8	77	66.9	56.1	40.3	14
DR041120HE02	69	61.7	53.1	44.4	58	52.2	48.3	36.5	11
DR041120HG02	158	68.4	68.4	69.5	134	66.1	63.1	62.2	24
DR041120HG06	199	80.03	76.41	66.4	179	72.7	66.3	60.3	20
DR041120HJ03	109	68.3	63.1	48.3	90	NR	NR	NR	NR
DR041120HJ28	99	61.4	58.9	49.9	56	55.0	49.5	37.6	43
DR041120HM01	79	66.7	54.9	44.5	58	55.3	55.4	33.7	21
DR041120HR01	58	47.9	51.7	36.6	47	43.1	49.7	31.2	11
DR041120HT03	135	74.6	69.0	53.8	118	69.8	64.7	47.0	17
UV042821HA04	NR	NR	NR	NR	NR	NR	NR	NR	NR
UV042821HA05	NR	NR	NR	NR	NR	NR	NR	NR	NR
UV042821HA11	69	58.3	50.6	46.9	56	54.4	47.0	42.7	13
UV042821HA12	121	69.9	64.4	56.0	NR	66.7	62.9	52.8	NR
UV042821HA22	125	67.8	64.1	59.6	109	59.5	61.9	59.0	16
UV042821HA31	94	65.1	59.1	43.5	62	63.0	49.9	39.0	32
UV042821HA34	38	49.4	49.0	27.6	18	43.6	37.7	19.2	20
UV042821HA46	78	75.1	50.1	42.2	58	67.9	43.8	39.2	20
UV042821HA48	67	82.1	63.1	22.1	43	74.5	55.5	16.0	24
UV042821HA52	76	59.6	56.5	51.9	53	55.7	49.6	36.6	23

*NR- Not Recorded

3.2 Hailstone melting and microplastic retrieval

All laboratory glassware, filtration equipment, and work surfaces were cleaned with Milli-Q® ultrapure water (18.2 MΩ), 70% isopropyl alcohol and stored in dust free cabinets when not in use. Filtration and sample preparation was conducted in a closed laboratory by a single researcher wearing a cotton laboratory coat to minimize airborne microplastic contamination. Each hailstone was rinsed individually with Milli-Q® water until all visible surface debris was removed. Due to the variability in hailstone size and morphology, rinsing time was not standardized but continued for some time beyond surface debris removal. Cleaned hailstones were placed in sterilized mason jars sealed with silicon paper and allowed to melt completely at room temperature. Meltwater was filtered immediately using a glass vacuum filtration system equipped with Whatman 47mm, 0.2µm filters (product no. 10417012) (Fig. 2). Filters were pre-

weighed using a Mettler Toledo AB265-S/FACT (± 0.1mg) analytical balance and visually inspected with a Leica M80 stereomicroscope prior to use. After filtration, filters were dried in covered Petri dishes, reweighed, and stored in airtight containers in dust free cabinets prior to analysis. To assess potential procedural contamination, blanks consisting of 100ml Milli-Q® water were processed at the beginning of the filtration cycle, after every tenth filtration, and at the end of the filtration cycle. No microplastics were detected in the blanks.

Figure 2. Vacuum filtration apparatus.

3.3 Spectroscopic identification of microplastics

Potential microplastic particles retained on filter membranes were identified initially via visual inspection using a Shimadzu optical microscope. Particles were categorized by morphology: fragments, fibers, films, or spheres and by color. Visual identification criteria followed established methods (Hartmann et al., 2019; Hidalgo-Ruz et al., 2012; Rochman et al., 2019).

A subset of visually identified particles was randomly selected by the researcher for polymer verification using a Shimadzu AIM-9000 FTIR microscope at the University of Texas Marine Science Institute. Transmission spectra were collected from 4000cm^{-1} to 400cm^{-1} at 8cm^{-1} resolution, averaging 36 scans per spectrum. The aperture was adjusted from 10 x 10 µm to 50 x 50 µm depending on the particle size to optimize signal to noise ratio.

Spectra were matched against the Shimadzu polymer reference library using the embedded LabSolutions IR software. A hit point score ≥ 564 (56.4%) was used as the threshold for polymer identification consistent with Akca et al. (2024). Identified polymers were classified into major categories (e.g., polycarbonate, epoxy, polybutadiene, polyethylene, polyamide, etc.). Matched hit points scores for microplastics examined in this study ranged between 564 and 787.

Color and morphological features were documented for each identified particle. Common colors included, red, orange, black, white, tan, gray, and green, consistent with prior atmospheric MP studies (Bergmann et al., 2019; Liu et al., 2019).

3.4 Statistical analysis

Given the non-normal distribution of the microplastic point scores and ordinal nature, non-parametric tests were employed. Differences in chemical species abundance across hailstones were evaluated using Krystal-Wallis H test, comparing median ranks, homoscedasticity and distributions among multiple independent groups.

Data was reshaped into long format, where each record represents individual hailstone MP chemical composition. The global rank (R_i) and sample size (n_i) were computed for each chemical group. The Kruskal–Wallis H test was calculated as:

$$H = \left(\frac{12}{N(N+1)}\right)\Sigma\left(\frac{R_i^2}{n_i}\right) - 3(N+1)$$

where N is the total number of valid observations across all groups. The resulting H-statistic was compared against a chi-square distribution with degrees of freedom equal to (k - 1), where k is the number of chemical groups. The chi square test was used with $\alpha = 0.05$. The test determined whether the polymer composition among hailstones differed significantly, indicating heterogeneity in source inputs or atmospheric transport processes.

3.5 HYSPLIT air mass back trajectory

The National Oceanic Atmospheric Administration (NOAA), Air Resources Laboratory HYSPLIT model was used to generate the 24-hour air mass back trajectories at eight hour intervals, using 1° x 1° Global Data Assimilation System (GDAS) datasets (Stein et al., 2015). Model starting coordinates corresponded to the convective core of each supercell: Del Rio (29°21′41″ N, 100°53′59″ W) and Uvalde (29°12′35″ N, 99°47′09″ W) and initiated from 0100 UTC 12 April 2020 and 0000 29 April 2021 respectively. Altitudes of 500m, 1500m, and 3000m above ground level (AGL) were considered in preliminary modeling and regional land-use influences because: the 500m is presumed to be the lowest altitude that atmospheric MPs would remain suspended and allow for transport without settling out, while the 1500m and 3000m AGL are the lower and upper boundary altitude of the low-level jet (LLJ) stream that may influence

the transport of MPs. Land-use classifications surrounding each storm track were derived from the ArcGIS on-line land-use dataset (2019). Areas were quantified by category (e.g., shrubland, cropland, urban, forest, grassland, and water bodies) to estimate the relative contribution of atmospheric microplastics by land-use.

3.6 Quality Assurance and Contamination Control

To minimize false positives, all sample preparation steps were performed under controlled conditions to minimize or eliminate MP contamination. Cotton laboratory apparel was used exclusively to avoid synthetic fiber shedding. Filtration blanks, clean laboratory conditions, and covered samples were maintained throughout processing. Glassware was used wherever possible, and all instruments were rinsed with ultrapure water between samples. Filters were visually inspected before and after filtration to confirm absence of background debris. The detection of microplastics in all hailstones but not in blanks supports the reliability of the analytical procedures.

4.0 Results and discussion

4.1 Microplastics in hailstones

Microplastics (MPs) were detected in all twenty-one hailstones analyzed, whereas *no* MPs were observed in procedural blanks, confirming that contamination was negligible (Fig. 3 & 4). Eleven hailstones collected from Del Rio yielded 125 MPs which included 5 natural particles and the ten hailstones from Uvalde yielded in 163 MPs and no natural particles (Fig. 5).

281

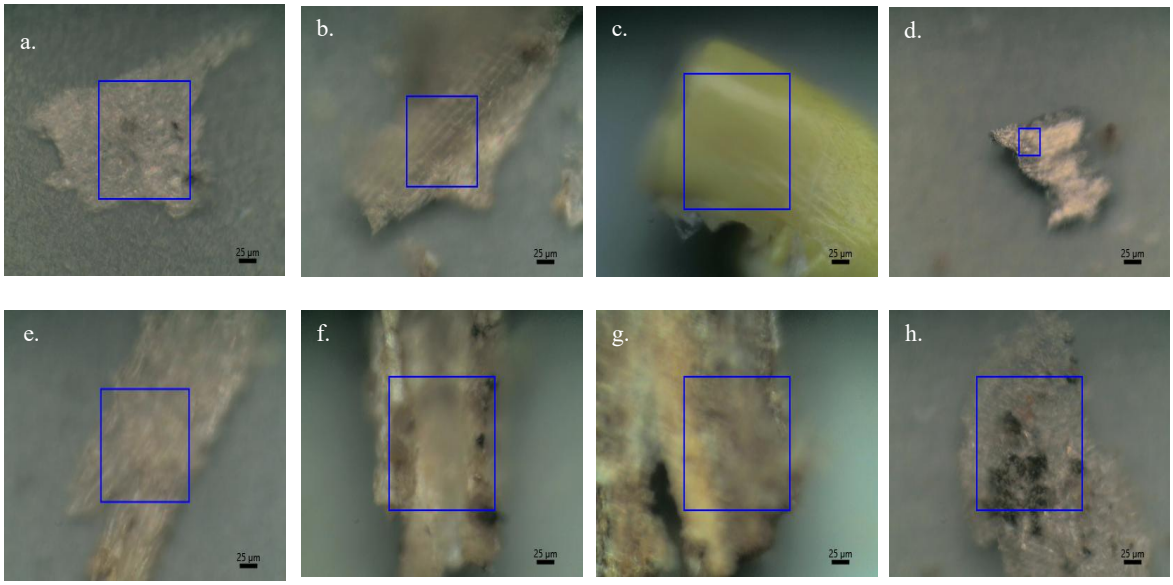

Figure 3. Microplastics viewed through Shimadzu micro FTIR, a.) UV042821HA48, Sample 10, score 787, low density polyethylene film, b.) DR041120HR01, Sample 5, score 729, polycarbonate, c.) UV042821HA52, sample 17, score 720, polycarbonate, d.) UV042821HA05, sample 22, score 718, polycarbonate, e.) UV042821HA52, sample 3, score 710, polycarbonate, f.) DR041120HE02, sample 8, score 708, polycarbonate, g.) DR041120HR01, sample 7, score 703, polycarbonate, h.) UV042821HA04, sample 7, score 702, polycarbonate.

282

283

284

285

286

287

288

289

290

291

292

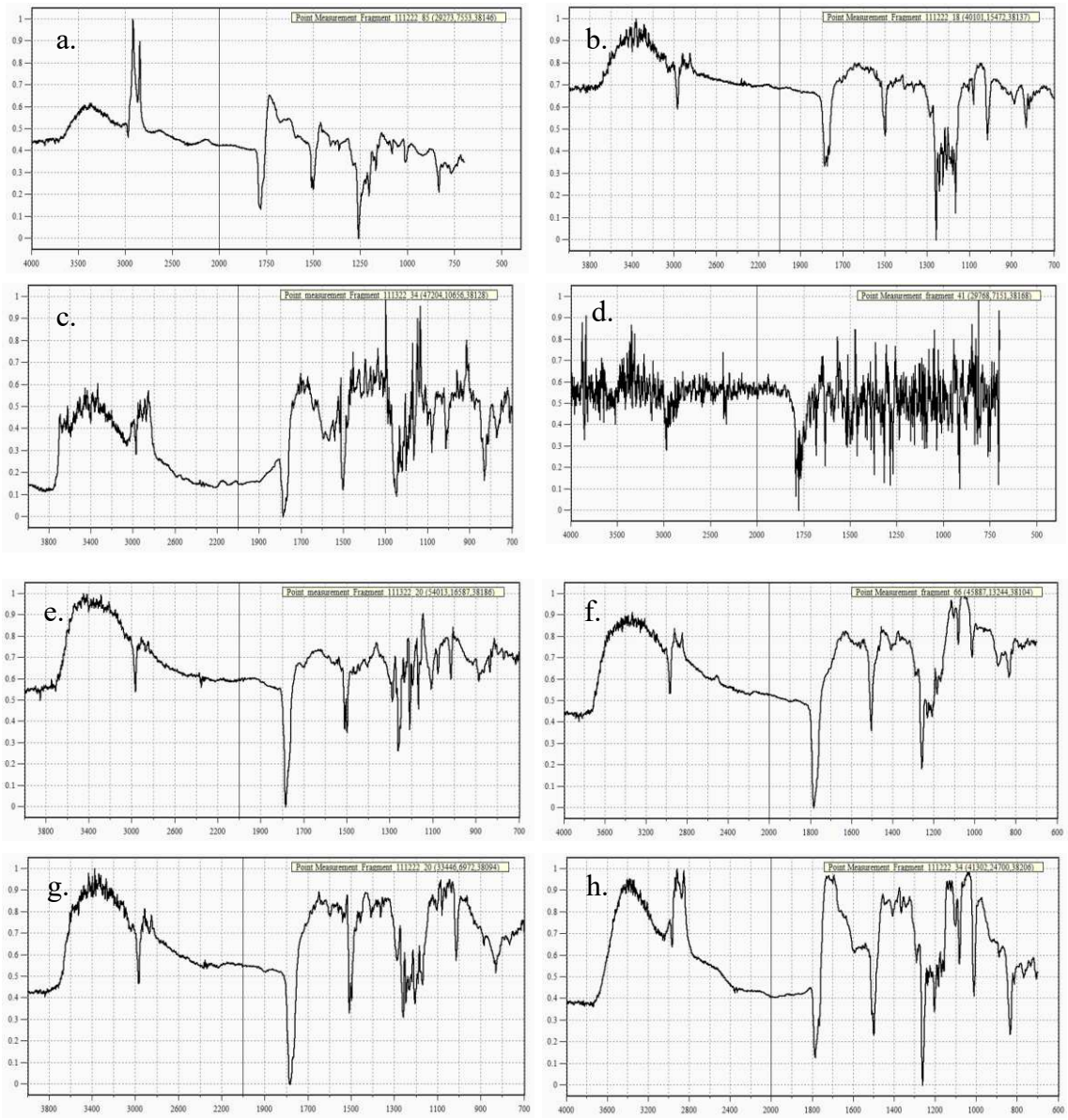

Figure 4. Spectra graphs of microplastics, a.) UV042821HA48, Sample 10, score 787, low density polyethylene film, b.) DR041120HR01, Sample 5, score 729, polycarbonate, c.) UV042821HA52, sample 17, score 720, polycarbonate, d.) UV042821HA05, sample 22, score 718, polycarbonate, e.) UV042821HA52, sample 3, score 710, polycarbonate, f.) DR041120HE02, sample 8, score 708, polycarbonate, g.) DR041120HR01, sample 7, score 703, polycarbonate, h.) UV042821HA04, sample 7, score 702, polycarbonate.

293

294

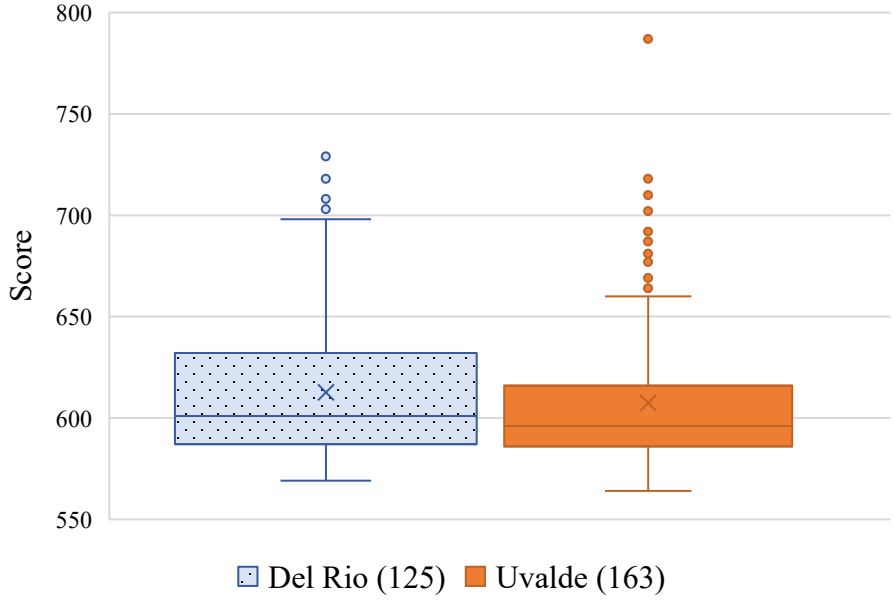

Figure 5. Shimadzu Lab Solutions IR software score by city (number of observations in parenthesis).

The highest number of MPs was recorded in hailstone UV042821HA05 (n = 21), whereas the lowest count was associated with hailstone DR041120HJ28 (n = 5). All filter membranes exhibited a high density of potential MPs, which constrained the feasibility of total particle identification within the allotted observation period. The number of MPs per hailstone ranged from 5 to 21, with an average of 13.7 ± 4.9 MP particles per sample.

These findings demonstrate that hailstones can serve as an effective natural collector of airborne MPs, preserving evidence of atmospheric pollution. The widespread presence of MPs, even in less industrialized regions, suggest that the majority of MPs were sourced primarily from proximal urban emission sources, with lesser contribution from long-range atmospheric transport within the troposphere (Allen et al., 2019; Brahney et al., 2020).

308

309 **4.2 Morphological characteristics**

310 Four primary morphological categories were identified: 200 fragments (69.4%), 68 fibers
311 (23.6%), 19 films (6.6%), and 1 sphere (0.4%). Fragments were by far the dominant shape,
312 consistent with mechanical weathering and photochemical degradation, breaking down
313 macroplastics into irregular shapes prior to atmospheric aerosolization (Dris et al., 2016; Klein
314 and Fischer, 2019). The prevalence of these "large" microplastics in both hail events provides
315 additional evidence of a more proximal emission source (Fig. 6).

316

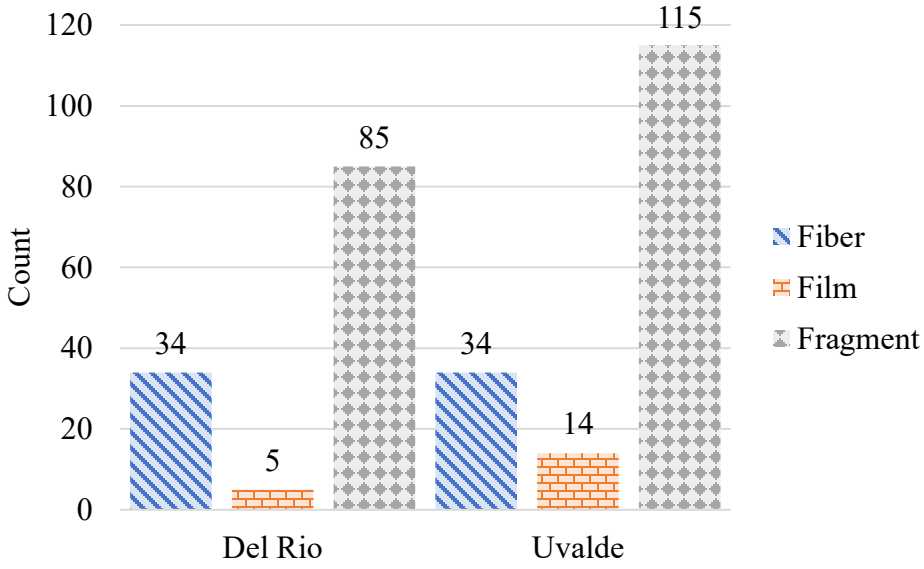

Figure 6. Microplastic shape by event location (one spherical particle from Uvalde has been excluded).

317

318 Per hailstone, the mean number of fragments observed was 9.71 ± 4.38, fibers 3.29 ± 2.99 and
319 0.9 ± 0.83 films, and only 1 spherical shape was observed in the entire sample population (Fig.
320 7). Assuming a uniform distribution of morphological shape categories, a Chi-square goodness-

of-fit test was performed to evaluate whether the distribution of MP shapes differed from a uniform distribution. The null hypothesis (H_0) assumed equal proportions across all categories ($p_{fiber} = p_{film} = p_{fragment} = p_{sphere} = 0.25$), while the alternative hypothesis (H_A) is that at least one shape is not equally proportional. The Chi-square goodness-of-fit test indicated a statistical significance that the distribution of MP shapes deviated from being equally proportional ($X^2 = 336.8$, $df = 3$, $\alpha = 0.05$, $p < 0.0001$), hence the null hypothesis was rejected.

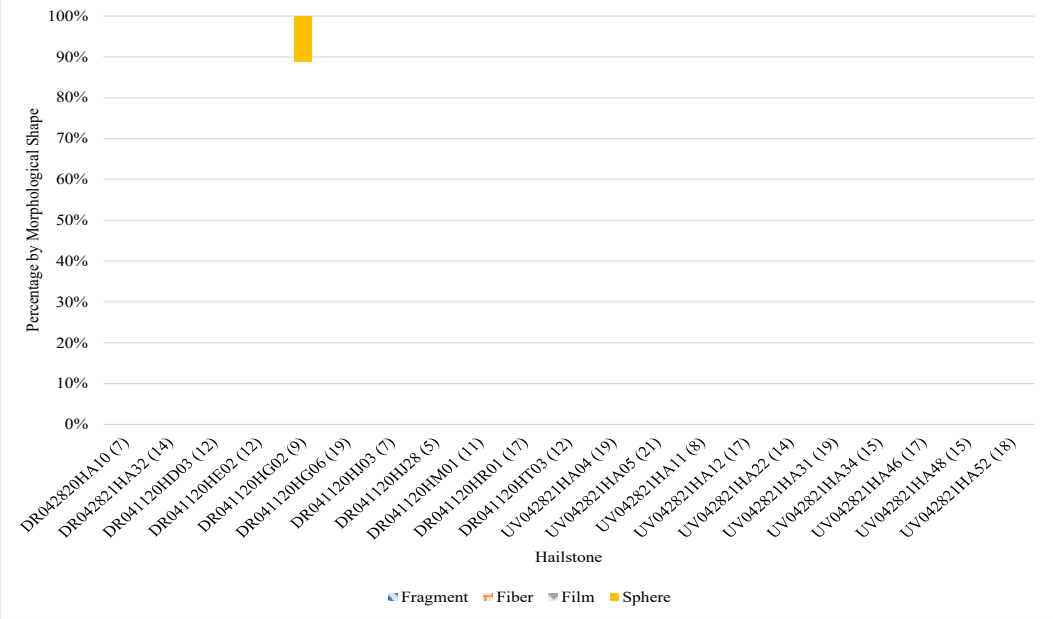

Figure 7. Microplastic shape morphology in individual hailstones. Parenthesis indicates number of microplastics analyzed.

The predominance of fragments reflects the extensive mechanical and photochemical degradation of plastics in urban emission source environments proximal to hail fall events, where abrasion and ultraviolet exposure facilitate fragmentation into angular particles capable of becoming airborne (Cooper and Corcoran, 2010; Steinmetz and Schröder, 2022). The scarcity of fibers could reflect the limited emission sources or the settling out over long distances of textile-derived materials whereas films and spheres likely experience higher aerodynamic drag,

reducing their atmospheric persistence (Liu et al., 2019; Xiao et al., 2023). These results are consistent with previous atmospheric and cryospheric studies that reported fragments dominate MP morphologies (Bergmann et al., 2019; Kozjek et al., 2023). It is believed that the predominance of these large MPs supports the contention that larger size MPs will be observed proximal to the emission source and that smaller fiber morphologies will be in greater abundance further from the emission source.

4.3 Microplastic chemical diversity

A total of 58 distinct polymer species were identified, 40 different species found in Del Rio hailstones and 48 species identified in Uvalde hailstones. The most prevalent polymers were polycarbonate (PC, n = 87), epoxy (EPX, n = 23), and polybutadiene (BR3, n = 14), together comprising over half (53.5%) of all confirmed MPs (Fig. 8). The top five chemical species for the Del Rio hailstones were polycarbonate (PC, n = 50), polybutadiene (BR3, n = 7), polymer additives (PA, n = 5), ramie (PLT, n = 5), and epoxy (EPX, n = 4), 56.8% of chemical species (Fig. 9). The top five chemical species for the Uvalde hailstones were polycarbonate (PC, n = 37), epoxy (EPX, n = 19), polymer additives (PA, n = 13), phenylene sulfide (PPS, n = 9), and polyimide (PI, n = 8), 52.8% of chemical species. See appendix A for a complete list of chemical species. These findings highlight the prevalence of polycarbonate (PC), epoxy (EPX), and polybutadiene (BR3) as the three most abundant chemical species with the balance of MPs representing a diverse array of synthetic and additive polymers across both hail events, underscoring the complexity and anthropogenic origin of MP contamination in convective storm systems. The chemical diversity of atmospheric MP contamination reflects a mixture of

359 industrial, urban, and agricultural sources supported by their presence in hailstones reenforcing
360 the ubiquity of MP atmospheric pollution.
361

362

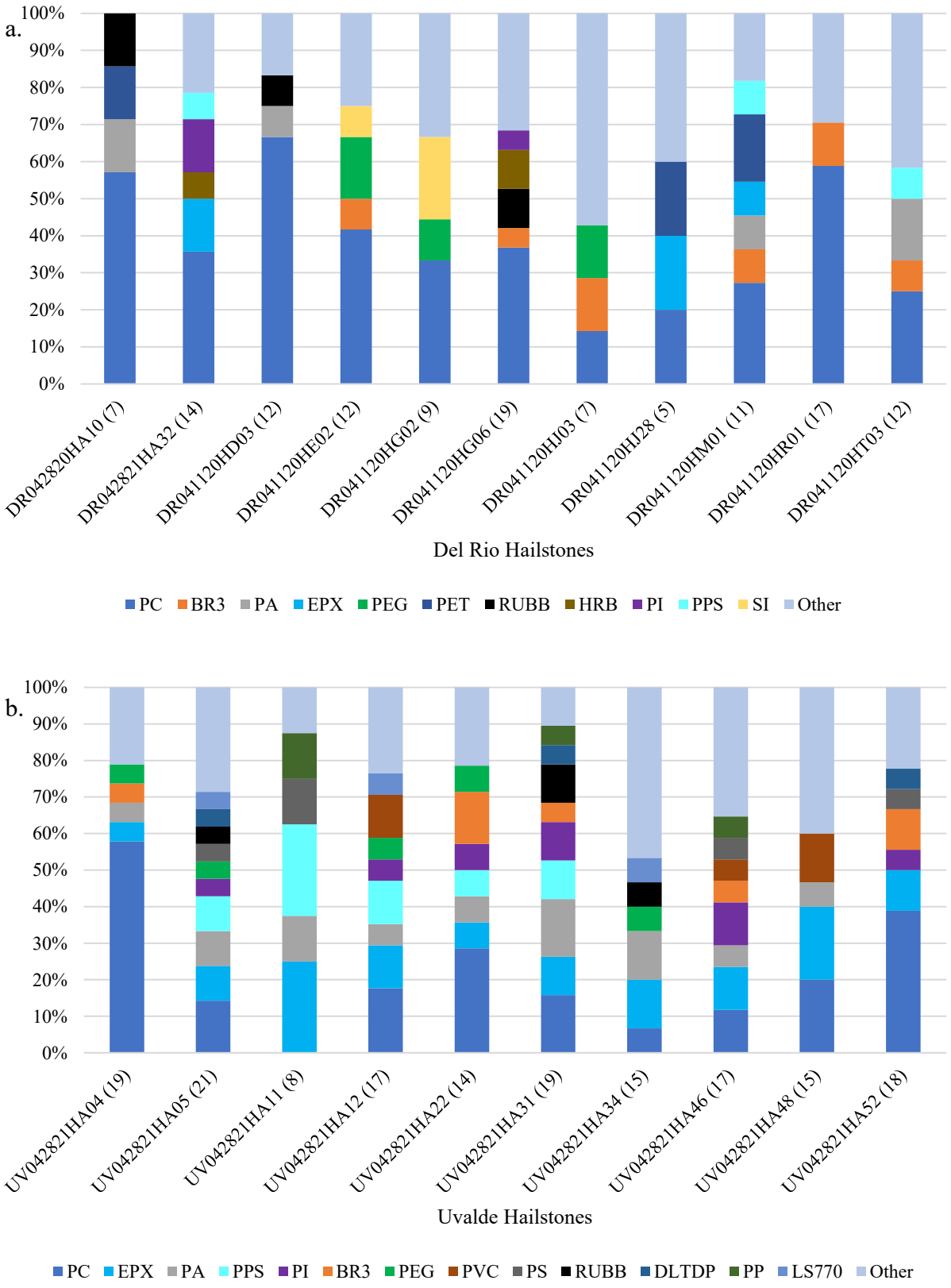

Figure 8. Chemical Species identified in hailstones, a) Del Rio and b) Uvalde.

363

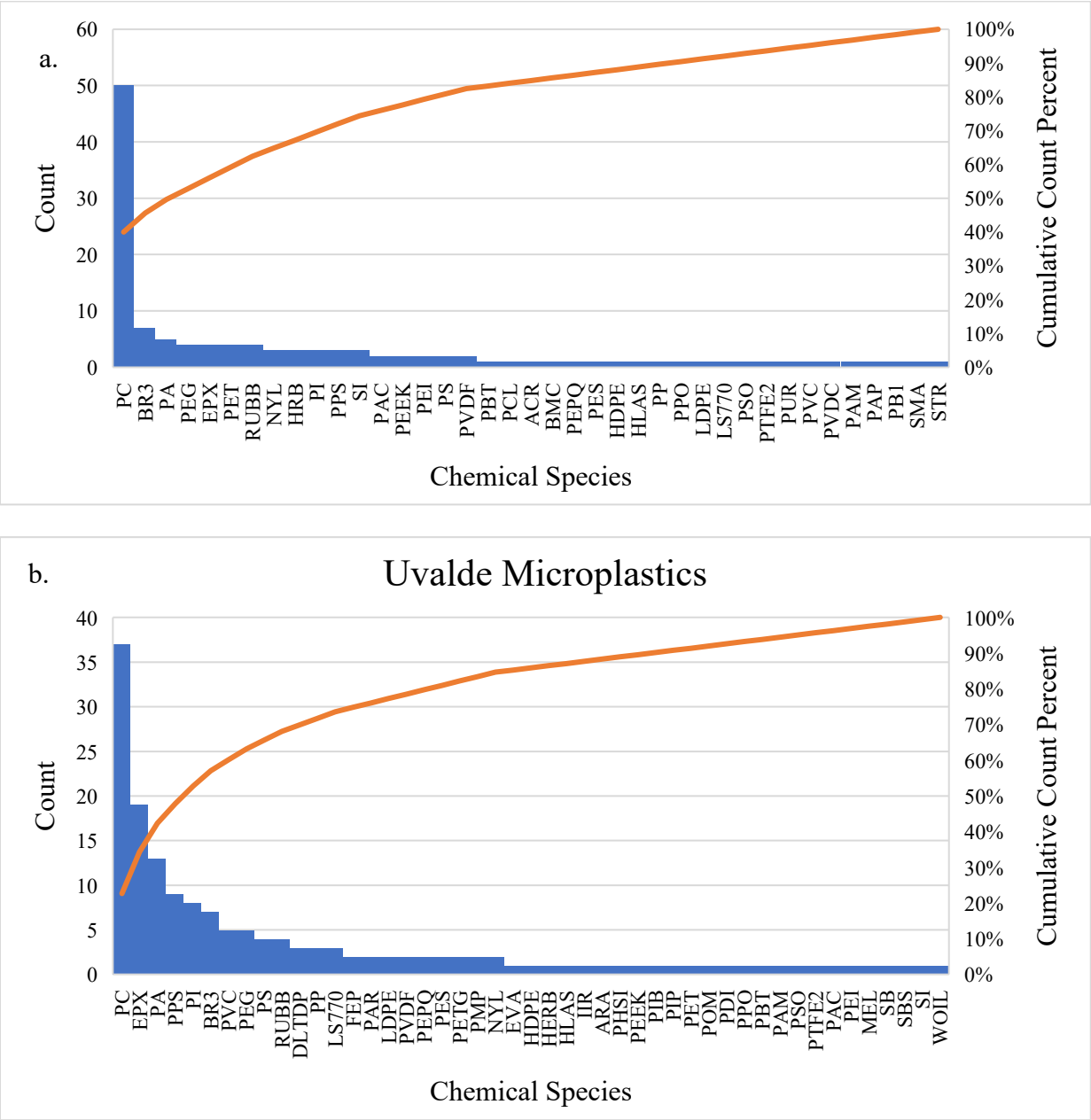

Figure 9. Pareto chart of a) Del Rio Texas and b) Uvalde Texas chemical species.

364

365 The Krustal – Wallis H test revealed a statistically significant difference among chemical species
366 (H = 80.7, df = 56, p = 0.0176), indicating compositional heterogeneity amongst hailstones. Such
367 variation likely reflects differing air-mass histories, emission intensities, and accretionary

processes during hailstone formation and growth. Denser or more hydrophilic polymers may preferentially nucleate or accrete onto hailstones, while lighter hydrophobic polymers may remain suspended for longer transport distances.

The MP diversity observed in this study aligns with other atmospheric MP research in urban and remote settings (Brahney et al., 2020; Chen et al., 2020; Kozjek et al., 2023). Higher concentrations of certain chemical species might result from their abundance in the surrounding terrestrial or urban environment, while other chemical species might be underrepresented resulting from degradation, transport distance or lower aerodynamic lifting potential. The polymer diversity observed among hailstones provides evidence that microplastic composition within convective systems reflects a proximal emission source for larger MPs while also supporting a spatially distributed emission source for lighter microplastics.

4.4 Source attribution and land-use influence: Del Rio case

Air-mass back trajectories indicate that the 500m AGL flow preceding the Del Rio event originated over the Gulf of America (Mexico), traversing the Rio Grande Valley before reaching the study area (Fig. 10 a & b). This pathway transits several population centers and manufacturing zones along the U.S. Mexico border, including McAllen, Laredo, and Eagle Pass. The U.S. side of the border has an estimated population of 485,000, while the population on the Mexican side is approximately 1,470,000 residents (Table 2). On the Mexican side, maquiladora manufacturing zones with operations in automotive, electronics, and consumer goods sectors represent likely emission sources of polycarbonate and epoxy-based polymers (Delphi Technologies, Panasonic, GE Aviation, Bosch, etc.) (Table 3).

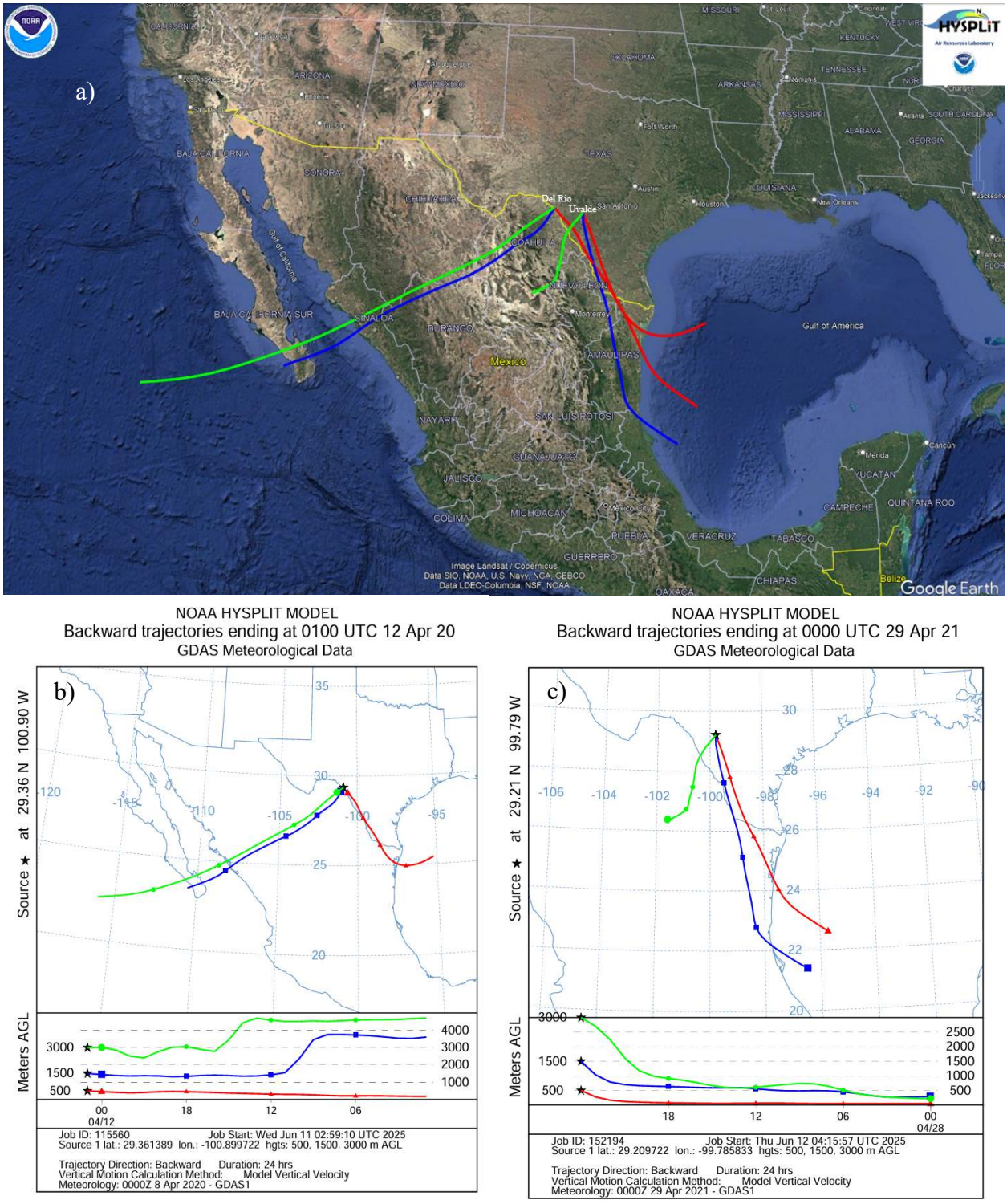

Figure 10. Back trajectory, a) air mass trajectories for both hail events, b.) Del Rio hail event, c.) Uvalde hail event.

392

393

Table 2. US and Mexico, city populations along air mass pathway.

United States				Mexico			
City	Population	Industries	Companies	City	Population	Industries	Companies
McAllen	149,000	Service Farming International Importing	Am - Mex Products	Reynosa	650,000	Automotive Electronics Metal Working	Delphi Technologies Panasonic LG Electronics
Laredo	259,000	Service International Importing	Concentrix	Nuevo Laredo	467,000	Automotive Electronics Consumer Goods	Panasonic Electrolux Continental Automotive Sys
Eagle Pass	28,000	Service	Kickapoo Lucky Eagle Casino	Piedras Negras	174,000	Automotive Electronics Aerospace Manufacturing	Aptiv Electrolux GE Aviation
Del Rio	48,000	Service Ranching United States Air Force	Laughlin Air Force Base	Ciudad Acuna	180,000	Automotive Electronics Aerospace Manufacturing	Bendix Cessna Bosch LG Electronics
				Monterrey	5,275,000	Aerospace Electronics Medical Devices Automotive	Lanix Electronics Femsa Cemex Groupo Alfa

394

395 Given the industrial activity and population of the Del Rio area, most larger MPs were likely
396 advected proximally to Del Rio via inflow boundary winds. In contrast, higher-altitude
397 trajectories (1500 - 3000m AGL) passed over sparsely populated desert terrain with limited
398 anthropogenic inputs, suggesting minimal contribution to hailstones from upper-level transport.
399 While it is possible that some lighter MPs were transported at higher altitudes, it is more
400 plausible that the majority of MPs observed in Del Rio hailstones originated from the Rio
401 Grande Valley and maquiladoras and were transported by lower-level (≤ 500 m) winds.

402

403 Land-use analysis further supports this interpretation: the source trajectory of Del Rio air masses
404 predominately traversed water bodies (38%), shrubland (19%), and forest (16%) (Table 3). The
405 limited cropland (1.8%) and urban footprint (0.2%) imply that local contributions were

406 significant relative to air mass atmospheric inputs. These findings highlight that even remote or
407 semi-rural areas may experience measurable atmospheric MP deposition due to aerosolization
408 resulting from inflow boundary winds and transport of MPs in air masses.
409

Table 3. Land-use

	Del Rio Area		Uvalde Area	
Land-use Description	Km^2	Percentage	Km^2	Percentage
Water Bodies	19,119	38.2%	7,162	20.7%
Shrubland	9,576	19.1%	10,469	30.3%
Conifer Forest	7,930	15.8%	4,944	14.3%
Mixed Vegetation	5,443	10.9%	5,013	14.5%
Mosaic Forest	3,340	6.7%	2,241	6.5%
Grassland Mosaic	1,878	3.8%	1,411	4.1%
Deciduous Forest	1,794	3.6%	2,179	6.3%
Croplands	879	1.8%	1,103	3.2%
Urban	88	0.2%	79	0.2%
	50,047	100.0%	34,601	100.0%

410

411 **4.5 Source attribution and land-use influence: Uvalde Case**

412 HYSPLIT trajectories of the Uvalde hail event show that the 500m AGL air mass similarly
413 originated from the Gulf of America (Mexico), making landfall near the Rio Grande and
414 progressing northward through urban border communities of the Rio Grande Valley (Fig. 9b).
415 The 1500m AGL air mass also originated in the Gulf of America (Mexico) south of the 500m
416 AGL, traversed the same direction and parallel to the 500m AGL air mass and passed east of
417 Monterrey, Mexico, a major industrial center (> 5 million inhabitants) with extensive

manufacturing in the electronics, aerospace, and medical device sectors. The 24-hr back trajectories of the 500m and 1500m AGL airmasses most likely contained a significant concentration of atmospheric MPs given the proximal pathway over anthropogenic emission sources. These air mass trajectories and anthropogenic inputs are plausible contributors to the abundance of polycarbonate, epoxy, and phenylene sulfide observed in Uvalde hailstones.

The 3000m AGL air mass trajectory traversed the Chihuahuan Desert, an area with low population density and minimal anthropogenic emission sources. Because the polymer composition (and size?) suggests local emission sources, there was limited contribution from high-altitude long-range transport.

Land-use of airmasses for the Uvalde hail event were comprised of shrubland (30%), water bodies (21%), forest (14%), mixed vegetation (15%), and cropland (3%) (Table 3). The combination of agricultural and light industrial activities, coupled with inflow air masses passing through the Rio Grande valley urban areas and maquiladoras of Mexico, supports a multi-source proximal MP signature consistent with previous studies linking land-use and atmospheric plastic loadings (Akca et al., 2024; Bi et al., 2023).

4.6 Environmental implications

The presence of MPs in every hailstone analyzed provides compelling evidence that microplastics are ubiquitous within the lower troposphere and can be efficiently scavenged by convective precipitation processes. Hailstones thus serve as valuable archival indicators of

atmospheric contamination, preserving both particle morphology and polymeric diversity within their layered structure.

The significant compositional heterogeneity among hailstones implies that atmospheric MPs originate from a complex mixture of emission sources, controlled by land-use type, population density, and meteorological inflow wind dynamics. Fragment-dominated morphologies suggest secondary microplastics derived from the degradation of larger debris sourced more proximal to the emission source rather than smaller morphologies sourced more distal from hail events.

This study demonstrates that severe weather events can play a critical role in distribution, aerosolization and deposition of airborne MPs, acting as an episodic sink within the global microplastic cycle. These findings extend the current understanding of atmospheric MP transport and support the use of hailstones as natural environmental samplers for future monitoring and model validation.

5.0 Conclusions

This study provides the first comprehensive evidence that hailstones act as natural archives of atmospheric microplastics. Every hailstone analyzed from two supercell thunderstorms in Texas contained microplastic particles, confirming that these contaminants are ubiquitous throughout the lower troposphere. The dominant morphology was fragments, reflecting extensive mechanical and photochemical degradation of larger plastics suspended or sweep aloft by inflow winds enhancing atmospheric particulate pollution. The most frequently detected polymers were

462 polycarbonate, epoxy, and polybutadiene which indicate strong contributions from
463 manufacturing, construction, and vehicular sources.
464
465 The statistically significant heterogeneity in polymer composition among hailstones suggests that
466 atmospheric microplastics originate from multiple, spatially proximal emission sources
467 controlled by land-use, population density, and manufacturing activity. Air-mass back-trajectory
468 analyses further demonstrate that inflow pathways along the Rio Grande Valley and
469 manufacturing zones along the border were likely sources of microplastics to the convective
470 storm event via inflow air masses. These findings provide direct evidence that convective storms
471 efficiently aerosolize and scavenge airborne microplastics, accreting them during repeated cycles
472 of hailstone growth.
473
474 Hailstones represent a previously underutilized medium for assessing atmospheric microplastic
475 pollution and transport. The layered accretion structure preserves both the diversity and spatial
476 variability of airborne particulates, providing new opportunities to trace emission sources and
477 atmospheric pathways. The results underscore the role of severe weather systems as episodic
478 sinks for airborne microplastics and highlight the importance of archiving hailstones for
479 research.
480
481 Future research should expand hailstone and precipitation sampling across different storm types,
482 and geography to better understand the mechanisms of microplastic entrainment, inflow
483 transport, and aerosolization. Future investigation of hailstones collected from regions with low
484 population density should be conducted to evaluate whether MP occurrence is minimal as

expected; if not, this could suggest that processes governing MP incorporation into hail are more ubiquitous and broadly applicable across diverse atmospheric environments globally. Spatial mapping of microplastic distribution within individual hailstones, combined with isotopic or chemical tracers, could further elucidate the coupling between land-use emissions and atmospheric microplastic cycling.

Acknowledgments

The authors thank the many citizen scientists for donating their collected hailstones to this study. We are encouraged by the enthusiasm of the young future scientists for their hailstone donations. This research was funded by NASA, the Center for Advanced Measurement in Extreme Environments (NASA grant #80NSSC19M0194) and the Center for Water Research at UTSA.

Supplemental Information

https://doi.org/10.5281/zenodo.19502758

References

Abbasi, S., Keshavarzi, B., Moore, F., Turner, A., Kelly, F. J., Dominguez, A. O., and Jaafarzadeh, N., 2019, Distribution and potential health impacts of microplastics and microrubbers in air and street dusts from Asaluyeh County, Iran: Environmental pollution, v. 244, p. 153-164.

Akca, M. O., Gündoğdu, S., Akca, H., Delialioğlu, R. A., Aksit, C., Turgay, O. C., and Harada, N., 2024, An evaluation on microplastic accumulations in Turkish soils under different land uses: Science of The Total Environment, v. 911, p. 168609.

Allen, J. T., Giammanco, I. M., Kumjian, M. R., Jurgen Punge, H., Zhang, Q., Groenemeijer, P., Kunz, M., and Ortega, K., 2020, Understanding hail in the earth system: Reviews of Geophysics, v. 58, no. 1, p. e2019RG000665.

Allen, S., Allen, D., Phoenix, V. R., Le Roux, G., Durántez Jiménez, P., Simonneau, A., Binet, S., and Galop, D., 2019, Atmospheric transport and deposition of microplastics in a remote mountain catchment: Nature Geoscience, v. 12, no. 5, p. 339-344.

514 Araujo, C. F., Nolasco, M. M., Ribeiro, A. M., and Ribeiro-Claro, P. J., 2018, Identification of
515 microplastics using Raman spectroscopy: Latest developments and future prospects:
516 Water research, v. 142, p. 426-440.
517 Bergmann, M., Mützel, S., Primpke, S., Tekman, M. B., Trachsel, J., and Gerdts, G., 2019, White
518 and wonderful? Microplastics prevail in snow from the Alps to the Arctic: Science
519 advances, v. 5, no. 8, p. eaax1157.
520 Bi, D., Wang, B., Li, Z., Zhang, Y., Ke, X., Huang, C., Liu, W., Luo, Y., Christie, P., and Wu, L.,
521 2023, Occurrence and distribution of microplastics in coastal plain soils under three land-
522 use types: Science of The Total Environment, v. 855, p. 159023.
523 Brahney, J., Hallerud, M., Heim, E., Hahnenberger, M., and Sukumaran, S., 2020, Plastic rain in
524 protected areas of the United States: Science, v. 368, no. 6496, p. 1257-1260.
525 Brahney, J., Mahowald, N., Prank, M., Cornwell, G., Klimont, Z., Matsui, H., and Prather, K. A.,
526 2021, Constraining the atmospheric limb of the plastic cycle: Proceedings of the National
527 Academy of Sciences, v. 118, no. 16, p. e2020719118.
528 Camarero, L., Bacardit, M., de Diego, A., and Arana, G., 2017, Decadal trends in atmospheric
529 deposition in a high elevation station: effects of climate and pollution on the long-range
530 flux of metals and trace elements over SW Europe: Atmospheric Environment, v. 167, p.
531 542-552.
532 Chen, G., Feng, Q., and Wang, J., 2020, Mini-review of microplastics in the atmosphere and their
533 risks to humans: Science of the Total Environment, v. 703, p. 135504.
534 Cheung, C. K. H., and Not, C., 2023, Impacts of extreme weather events on microplastic
535 distribution in coastal environments: Science of The Total Environment, v. 904, p.
536 166723.
537 Cooper, D. A., and Corcoran, P. L., 2010, Effects of mechanical and chemical processes on the
538 degradation of plastic beach debris on the island of Kauai, Hawaii: Marine pollution
539 bulletin, v. 60, no. 5, p. 650-654.
540 Dris, R., Gasperi, J., Mirande, C., Mandin, C., Guerrouache, M., Langlois, V., and Tassin, B.,
541 2017, A first overview of textile fibers, including microplastics, in indoor and outdoor
542 environments: Environmental pollution, v. 221, p. 453-458.
543 Dris, R., Gasperi, J., Saad, M., Mirande, C., and Tassin, B., 2016, Synthetic fibers in atmospheric
544 fallout: a source of microplastics in the environment?: Marine pollution bulletin, v. 104,
545 no. 1-2, p. 290-293.
546 Gasperi, J., Wright, S. L., Dris, R., Collard, F., Mandin, C., Guerrouache, M., Langlois, V., Kelly,
547 F. J., and Tassin, B., 2018, Microplastics in air: are we breathing it in?: Current Opinion
548 in Environmental Science & Health, v. 1, p. 1-5.
549 Habib, R. Z., Al Kendi, R., Ghebremedhin, F., Elkashlan, M., Iftikhar, S. H., Poulose, V.,
550 Ramachandran, T., Mourad, A.-H. I., Hamed, F., and Thiemann, T., 2022, Tire and rubber
551 particles in the environment—A case study from a hot arid region: Frontiers in
552 Environmental Science, v. 10, p. 1009802.
553 Habibi, N., Uddin, S., Behbehani, M., and Lee, J.-Y., 2024, Is atmospheric pathway a significant
554 contributor to microplastics in the marine environment?: Emerging Contaminants, v. 10,
555 no. 2, p. 100297.
556 Hartmann, N. B., Hüffer, T., Thompson, R. C., Hassellöv, M., Verschoor, A., Daugaard, A. E.,
557 Rist, S., Karlsson, T., Brennholt, N., Cole, M., Herrling, M. P., Hess, M. C., Ivleva, N. P.,
558 Lusher, A. L., and Wagner, M., 2019, Are We Speaking the Same Language?

559 Recommendations for a Definition and Categorization Framework for Plastic Debris:
560 Environmental Science & Technology, v. 53, no. 3, p. 1039-1047.
561 Hidalgo-Ruz, V., Gutow, L., Thompson, R. C., and Thiel, M., 2012, Microplastics in the marine
562 environment: a review of the methods used for identification and quantification:
563 Environmental science & technology, v. 46, no. 6, p. 3060-3075.
564 Huang, Y., He, T., Yan, M., Yang, L., Gong, H., Wang, W., Qing, X., and Wang, J., 2021,
565 Atmospheric transport and deposition of microplastics in a subtropical urban
566 environment: Journal of Hazardous Materials, v. 416, p. 126168.
567 Klein, M., and Fischer, E. K., 2019, Microplastic abundance in atmospheric deposition within the
568 Metropolitan area of Hamburg, Germany: Science of the Total Environment, v. 685, p.
569 96-103.
570 Knight, C., Knight, N., Brooks, H. E., and Skripnikova, K., 2019, Hail and Hailstorms☆,
571 Reference Module in Earth Systems and Environmental Sciences, Elsevier.
572 Kozjek, M., Vengust, D., Radošević, T., Žitko, G., Koren, S., Toplak, N., Jerman, I., Butala, M.,
573 Podlogar, M., and Viršek, M. K., 2023, Dissecting giant hailstones: A glimpse into the
574 troposphere with its diverse bacterial communities and fibrous microplastics: Science of
575 the Total Environment, v. 856, p. 158786.
576 Law, K. L., and Thompson, R. C., 2014, Microplastics in the seas: Science, v. 345, no. 6193, p.
577 144-145.
578 Li, X., Zhang, Q., Zhou, L., and An, Y., 2020, Chemical composition of a hailstone: evidence for
579 tracking hailstone trajectory in deep convection: Science Bulletin.
580 Liu, K., Wang, X., Fang, T., Xu, P., Zhu, L., and Li, D., 2019, Source and potential risk
581 assessment of suspended atmospheric microplastics in Shanghai: Science of The Total
582 Environment, v. 675, p. 462-471.
583 Nordstrand, T. E., 2021, Characterization of Large Hailstone Growth Using Stable Isotopes: The
584 University of Texas at San Antonio.
585 Peng, J., Wang, J., and Cai, L., 2017, Current understanding of microplastics in the environment:
586 occurrence, fate, risks, and what we should do: Integrated environmental assessment and
587 management, v. 13, no. 3, p. 476-482.
588 Prata, J. C., 2018, Airborne microplastics: consequences to human health?: Environmental
589 pollution, v. 234, p. 115-126.
590 Raupach, T. H., Martius, O., Allen, J. T., Kunz, M., Lasher-Trapp, S., Mohr, S., Rasmussen, K.
591 L., Trapp, R. J., and Zhang, Q., 2021, The effects of climate change on hailstorms: Nature
592 Reviews Earth & Environment, v. 2, no. 3, p. 213-226.
593 Rochman, C. M., Brookson, C., Bikker, J., Djuric, N., Earn, A., Bucci, K., Athey, S., Huntington,
594 A., McIlwraith, H., and Munno, K., 2019, Rethinking microplastics as a diverse
595 contaminant suite: Environmental toxicology and chemistry, v. 38, no. 4, p. 703-711.
596 Šantl-Temkiv, T., Finster, K., Dittmar, T., Hansen, B. M., Thyrhaug, R., Nielsen, N. W., and
597 Karlson, U. G., 2013, Hailstones: A Window into the Microbial and Chemical Inventory
598 of a Storm Cloud: PLOS ONE, v. 8, no. 1, p. e53550.
599 Song, Y. K., Hong, S. H., Jang, M., Han, G. M., Rani, M., Lee, J., and Shim, W. J., 2015, A
600 comparison of microscopic and spectroscopic identification methods for analysis of
601 microplastics in environmental samples: Marine pollution bulletin, v. 93, no. 1-2, p. 202-
602 209.

Stanton, T., Johnson, M., Nathanail, P., MacNaughtan, W., and Gomes, R. L., 2019, Freshwater and airborne textile fibre populations are dominated by 'natural', not microplastic, fibres: Science of the total environment, v. 666, p. 377-389.

Stein, A. F., Draxler, R. R., Rolph, G. D., Stunder, B. J., Cohen, M. D., and Ngan, F., 2015, NOAA's HYSPLIT atmospheric transport and dispersion modeling system: Bulletin of the American Meteorological Society, v. 96, no. 12, p. 2059-2077.

Steinmetz, Z., and Schröder, H., 2022, Plastic debris in plastic-mulched soil—a screening study from western Germany: PeerJ, v. 10, p. e13781.

Temkiv, T. Š., Finster, K., Hansen, B. M., Nielsen, N. W., and Karlson, U. G., 2012, The microbial diversity of a storm cloud as assessed by hailstones: FEMS microbiology ecology, v. 81, no. 3, p. 684-695.

Thompson, R. C., Olsen, Y., Mitchell, R. P., Davis, A., Rowland, S. J., John, A. W., McGonigle, D., and Russell, A. E., 2004, Lost at sea: where is all the plastic?: Science, v. 304, no. 5672, p. 838-838.

Worm, B., Lotze, H. K., Jubinville, I., Wilcox, C., and Jambeck, J., 2017, Plastic as a persistent marine pollutant: Annual Review of Environment and Resources, v. 42, no. 1, p. 1-26.

Xiao, S., Cui, Y., Brahney, J., Mahowald, N. M., and Li, Q., 2023, Long-distance atmospheric transport of microplastic fibres influenced by their shapes: Nature Geoscience, v. 16, no. 10, p. 863-870.

Zhang, Y., Kang, S., Allen, S., Allen, D., Gao, T., and Sillanpää, M., 2020, Atmospheric microplastics: A review on current status and perspectives: Earth-Science Reviews, v. 203, p. 103118.

Supplementary Files

This is a list of supplementary files associated with this preprint. Click to download.

- S1DelRioHailstoneFTIRData.pdf
- S2UvaldeHailstoneFTIRData.pdf
- S3DataStatisticsandGraphics.xlsx
- S4MicroplasticsDataMaster2022MicroFTIRManuscript.xlsx
- S5KrustalWallisSubmissionSupplementalInfo.xlsx